

A Study of Optical and Thermal Properties of ($TeO_2 - MoO_3 - ZnO$) Semiconducting Oxid Glass

Nadher A. Ali, AbdulKarim Z. Khalf, Manaf A. Hassan

physics Department , college of education for pure sciences, University of Kirkuk, Iraq

nadherahmed97@gmail.com

<https://orcid.org/0009-0008-2159-1440>

ABSTRACT

produced a standard series of semiconducting tellurite oxide glasses containing vanadium and molybdenum oxides based on $(65\%TeO_2 - (35 - x)\%MoO_3 - x\%ZnO)$, where $X = 10, 15, 20, 25, 30$ (mol-%) including quenching method. The influence of MoO_3 on the glass transition temperature and photofission energy of this kind was analyzed. The thermal parameters of the used glasses, such as transition temperature (T_g) and thermal stability, were measured using the differential scanning calorimetry (DSC) method. Optical gap energy (E_{opt}) and end (E_o) were evaluated as a function of (ZnO) content in the glass. It was found that E_{opt} decreased with the increase of ZnO content, while ZnO content increased. Infrared and Raman spectroscopy, X-ray diffraction and scanning electron microscopy were examined and analyzed as a function of ZnO content in different compositions of such glasses.

Keywords: Tellurite glasses; Optical band gap; XRD; Raman Spectra; FTIR; DSC

1. Introduction

Many researchers have analyzed oxide glasses with different metal oxides [1-3]. Among oxide glasses with high power, glass has high refractive index and high vitrification power. Glasses with high tellurium oxide content exhibit interesting thermal and physical properties [4]. The effect of several transition metal oxide modifiers on thermal stability has been analyzed [5]. Changes in glass composition can affect induced light absorption due to non-bridging oxygen content [6]. The study of DSC and structural properties of oxide glasses is a good way to study the behavior of such glasses as a function of different compositions [7]. Thermal stability and glass transition temperature were analyzed using differential scanning calorimetry technique [8]. In the present work, we investigate different parameters of different glass network compositions, such as transition temperature (T_g), optical gap energy, energy band position, and Raman shift.

2. Experimental procedure

Glasses of the $TeO_2 - MoO_3 - ZnO$ system were fabricated according to standard methods with a total bath weight of 30 g. Heat the melt in a deep alumina crucible at $(700-900)$ °C for one hour. The identification of glass samples at a heating rate of 10 °C/min in the $(20-600)$ °C range using (PANalytical) X-ray diffraction and differential scanning of glass samples has been reported. Infrared absorption measurements in the $(400-4000)$ cm⁻¹ range. Absorption spectra in the wavelength range $(200-900)$ nm were studied at room temperature.

3. Resulting and discussion

3.1 Spectra of X-ray diffraction

The X-ray diffraction patterns of ($65\% TeO_2 - 15\% MoO_3 - 20\% ZnO$) samples are shown in Figure 1. As can be seen from the figure, there are no discrete peaks, indicating that the glass sample examined is amorphous.

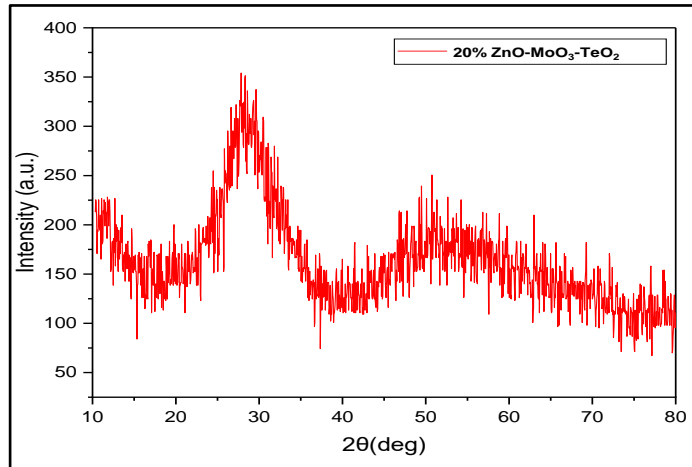


Figure.1: XRD spectra of ($65\% TeO_2 - 15\% MoO_3 - 20\% ZnO$)

3.2 Optical absorption spectra

The optical absorption spectra of $TeO_2 - MoO_3 - ZnO$ glasses system are shown in Figure.2

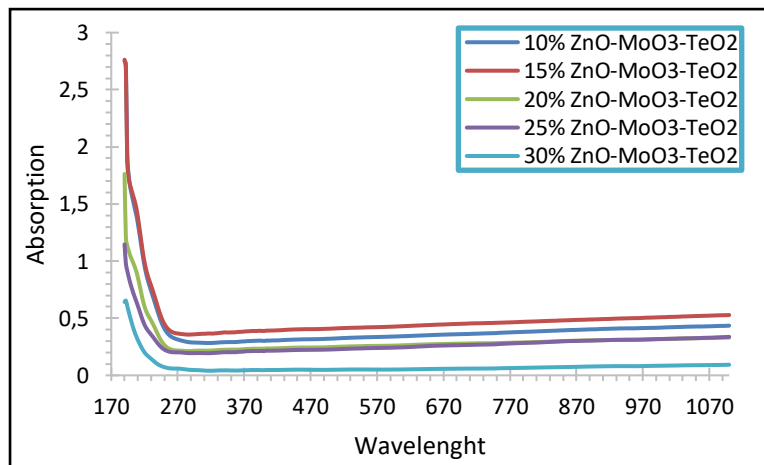


Figure.2 Optical absorption of $TeO_2 - MoO_3 - ZnO$ glass system

As can be seen from the absorption end, the intensity versus wavelength absorption coefficient $\alpha(\omega)$ is evaluated by the following relationship:

$$\alpha(\omega) = \frac{1}{d} \ln \left(\frac{I}{I_t} \right) \quad \dots \dots \dots \quad (1)$$

where (d) represents the thickness of the sample, and $\ln \left(\frac{I}{I_t} \right)$ is related to the absorbance (A). Energy is calculated by the formula $E = \hbar\omega$. The optical gap energy (E_{opt}) and the absorption coefficient $\alpha(\omega)$ are

related by equation [10].

$$\alpha(\omega) = B \frac{(\hbar\omega - E_{opt})^r}{(\hbar\omega)} \quad \dots \dots \dots \quad (2)$$

where (B) is a constant and (r) has a value based on the energy band transition mechanism. For indirect transformations (r=2). The relationship between (E_{opt}) and the refractive index (n) is determined by formula [11].

$$\left[\frac{n^2 - 1}{n^2 + 2} \right] = 1 - \sqrt{\frac{E_{opt}}{20}} \quad \dots \dots \dots \quad (3)$$

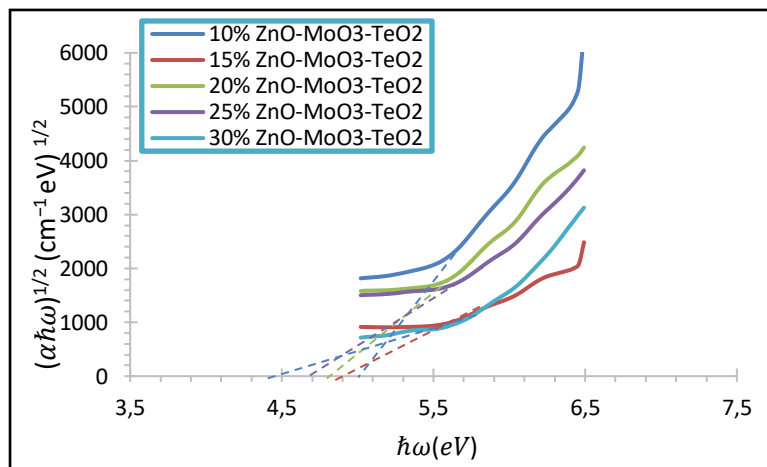


Figure.3 $(\alpha\hbar\omega)^{\frac{1}{2}}$ quantity as a function of photon energy of ($\text{TeO}_2 - \text{MoO}_3 - \text{ZnO}$)

Fig.3 shows a graph between the photon energy $\alpha(\omega)$ and the quantity $(\alpha\hbar\omega)^{\frac{1}{2}}$. Band gap (E_{opt}) of each sample is determined from Fig.3 by extrapolating the straight portion of the $(\alpha\hbar\omega)^{\frac{1}{2}}$ versus $(\hbar\omega)$ plot on the $(\hbar\omega)$ axis at $(\alpha\hbar\omega)^{\frac{1}{2}} = 0$. The Optical energy values of glass samples were plotted as a function of ZnO content are shown in Figure 4.

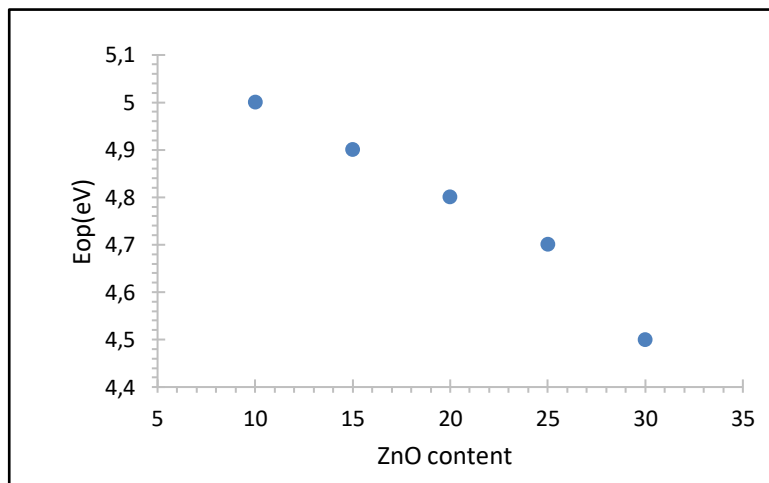


Figure.4. Variation of (E_{opt}) with ZnO concentration ($\text{TeO}_2 - \text{MoO}_3 - \text{ZnO}$)

It can be seen from Figure 4. It is shown that (E_{opt}) decreases with the increase of ZnO concentration in the amorphous system, and it is found that the energy band ends at the forbidden band. The strength of

these bands is related to the perturbation and can be calculated using Urbach's formula. For most amorphous and crystalline materials, the absorption coefficient $\alpha(\omega)$ is exponential with $\hbar\omega$. The known exponential change from Urbach's formula can be given by [12].

$$\alpha(\omega) = \alpha_0 \exp\left(\frac{\hbar\omega}{E_0}\right) \quad \dots \quad (4)$$

The Urbach curve of the tested glasses is shown in Figure 5.

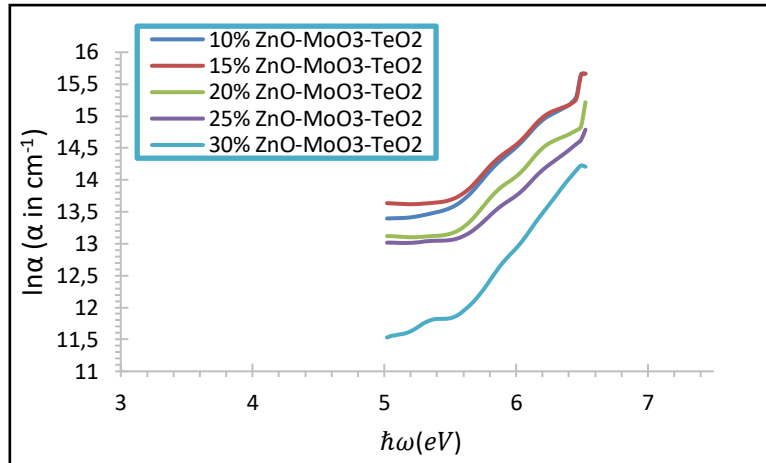


Figure.5. Urbach plots of $TeO_2 - MoO_3 - ZnO$

The reciprocal of the slopes measure the energy of band tails (E_o).

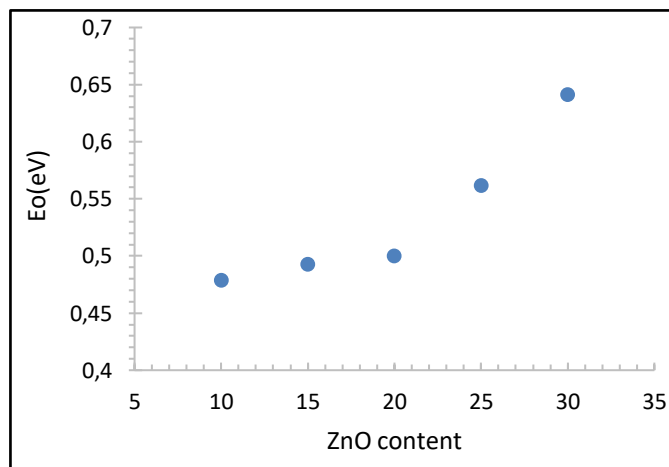


Figure.6. Band tails energy as a function of ZnO content in $TeO_2 - MoO_3 - ZnO$ glass system

The variation of band tails (E_o) with the increasing of ZnO concentrations are shown in figure.6.

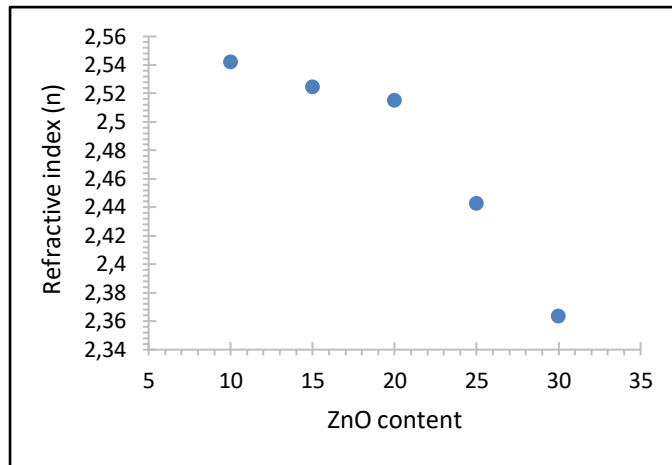


Figure.7. Variations of refractive index (n) with ZnO content in $TeO_2 - MoO_3 - ZnO$ glass system

Figure.7. Shows the decreasing of estimated (n) with of ZnO content.

Table (1): Optical parameters of $TeO_2 - MoO_3 - ZnO$

ZnO Content	$E_{opt}(eV)$	$E_o(eV)$	Refractive Index(n)
10	5	0.47	2.542
15	4.9	0.492	2.524
20	4.8	0.5	2.514
25	4.7	0.56	2.442
30	4.5	0.641	2.363

Table (1). Shows the values of E_{opt} , E_o and n with increasing of ZnO content in the glass system

3.3. Differential Scanning Calorimetry

The DSC curve of the $TeO_2 - MoO_3 - ZnO$ glass system is shown in Figure 8. The thermal interpretation of the glass system was performed from room temperature to 600 °C at an interval of 10 °C/min. The transition temperature (Tg) and stability (S), crystallization temperature (Tc) and thermodynamic fragility (F) were calculated and listed in Table (2).

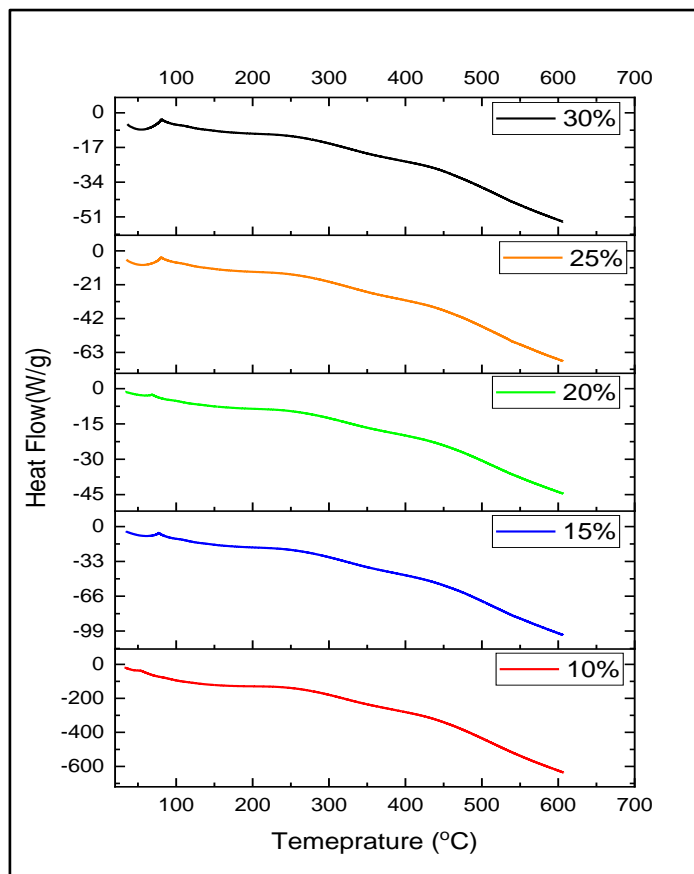


Figure.8. DSC plots of $TeO_2 - MoO_3 - ZnO$ glass system

Table (2): Values of differential thermal parameters of $TeO_2 - MoO_3 - ZnO$ glass system

ZnO content	Tg	Tc	F	S
10%	240	416	0.266247	18.33333
15%	245	425	0.298184	16.16327
20%	246	428	0.235194	16.27642
25%	248	430	0.162115	14.67742
30%	248	422	0.218852	11.92742

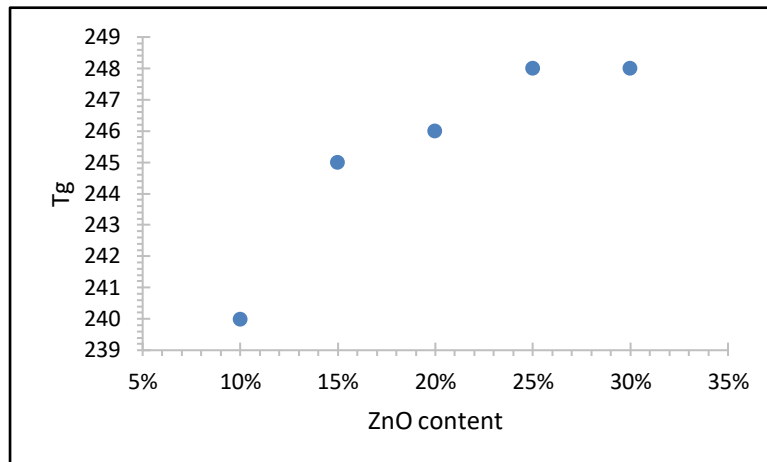


Figure.9. Variation of transition temperature (T_g) with MoO_3 content in $\text{TeO}_2 - \text{MoO}_3 - \text{ZnO}$ glass system

As shown in Table (2), the variation of the DSC curves in Figure.9. where crystallization is clearly heat-emitting after the glass transition temperature, which indicates the nature of the glassy state of the material at a temperature lower than the glass transition temperature, and the glass transition temperature (T_g) increases from (240 – 248)°C with an increase in the concentration of ZnO in the glass system from 10 mol% to 30 mol%. The T_c values range between (430 – 416) °C and the reason for the increase in the crystallization temperature is due to the reduction of the spacing between the ZnO atoms. The thermal stability decreases from 18.333 to 11.927 with an increase of 30 mol% ZnO content as shown in Figure.10.[13,14]

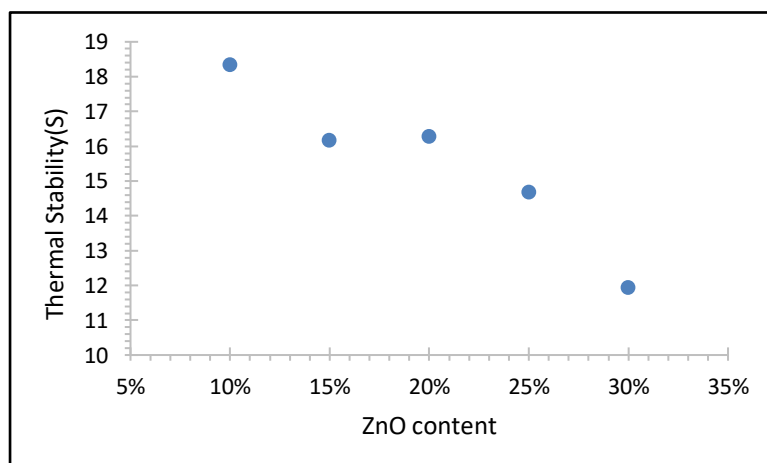


Fig.10. Variation of the thermal stability with ZnO content in $\text{TeO}_2 - \text{MoO}_3 - \text{ZnO}$ glass system.

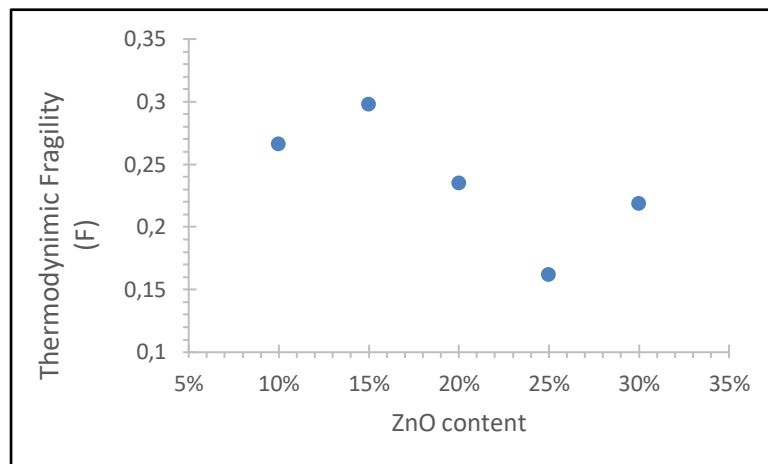


Figure.11. Variation thermodynamic fragility with MoO_3 content in $\text{TeO}_2 - \text{MoO}_3 - \text{ZnO}$ glass system

The glassy compound (ZnO) as shown in Figure.11. shows that the fragility decreases with an increase in the percentage of (ZnO) from 15% to 25% and causes disturbances, and this leads to the formation of non-bridging oxygen's in thermodynamic fragility.

3.4 Raman Spectra

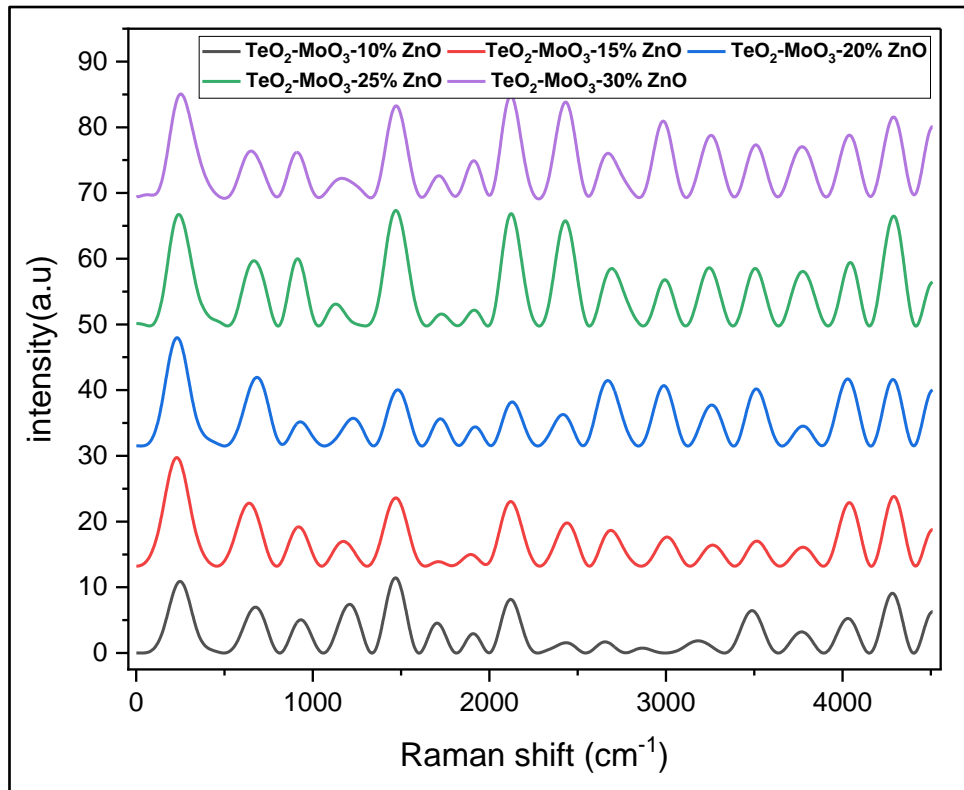


Figure.12. Raman Spectra of $\text{TeO}_2 - \text{MoO}_3 - \text{ZnO}$ glass system

Table (3): Raman bands position of the $\text{TeO}_2 - \text{MoO}_3 - \text{ZnO}$

ZnO content	Raman Shift(cm^{-1})				
10%	247	675	933	1208	1469
15%	229	639	920	1172	1469
20%	232	683	928	1229	1482
25%	239	667	912	1129	1469
30%	252	649	910	1165	1471

The Raman beam at (229-252) cm^{-1} is attributed to the distortion of the vibrational modes of an O – Te – O conducting oxygen-containing glass lattice [15]. As for the Raman beam (649-683) cm^{-1} resulting from the symmetric vibrational modes of TeO_4 and the bonding (Te – O – Zn)[16, 17]. The Raman beam at (910-933) cm^{-1} is caused by the vibrations of the Mo – O bond [18]. Also, the beam at (1129-1208) cm^{-1} refers to the stretching of the vibrations of the Te – O – Zn bonds [16], while the Raman beam at (1469-1482) cm^{-1} refers to the stretching of the Mo – O bonds associated with different groups [19].

3.5 Infrared absorption spectra

Figure. 13. IR absorption spectra of $\text{TeO}_2 - \text{MoO}_3 - \text{ZnO}$ glass system

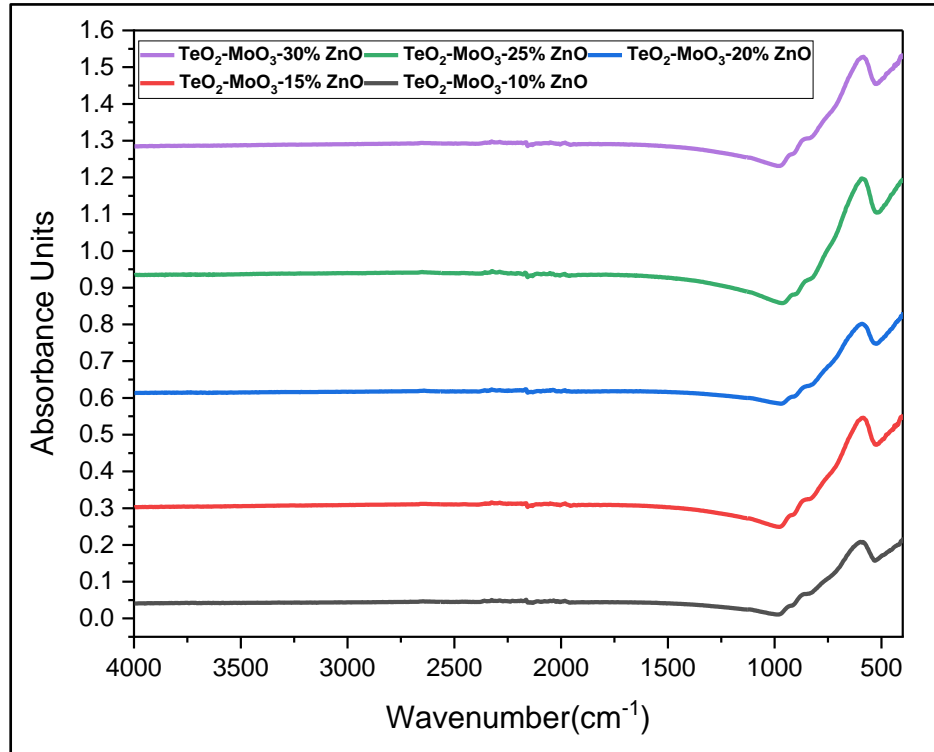


Table (4): Band position of $\text{TeO}_2 - \text{V}_2\text{O}_5 - \text{MoO}_3$ glass system

ZnO content	Band position(cm^{-1})			
	500	800	900	1900
10	530	833	921-982	1958
15	527	835	914-983	1959
20	521	837	908-970	
25	518	829	905-965	
30	515	823-894	953	

Figure.13. and Table (4) show the infrared absorption of the glass system within the range (400-2000) cm^{-1} . As shown in the figure, there are four vibration bands that include the structure of tellurium (Te) and molybdenum (Zn): at (500, 800, 900, 1900) cm^{-1} . It was found that there is a band between (515-530) cm^{-1} , due to the multi-bonds of the Te – O – Te bridges. It was also found that at the same frequency, wide bands due to the Si – O – Si bridges [16]. There is also a band between cm^{-1} (823-894), which is attributed to the Mo – O – Mo bond [20]. We also note that with the increase in the percentage of ZnO, there was a band at cm^{-1} (905-982), which refers to the Mo – O bond and the Mo = O bond in MoO_4 units [18]. As for the band (1958,1958) cm^{-1} , it was encoded to the symmetric Te – O bond tetrahedron of TeO_4 units [21].

References

1. D. Souri and S.A Salehizadeh, J.Mater.Sci. 44,5800(2009).
2. D.Souri and K. Shomalian, J. Non – Cryst. Solid. 335,1597 (2009).
3. D. Souri, J. phys. D Appl. Phys. 41,105102(2008).
4. I. Saveleii, Jc. Jules, G. Gadret, and B.Kibler, Opt. Mater. 33, 1661(2011).
5. J. Yne, T. Xue, F.itung , J. Non – cryst . Solids , 408, 1 – 6 (2015).
6. G. Turky and M. Dawy, Mater. Chem. Phys, 77, 48(2002).
7. G.W. Scherer, Relaxation in Glasses and composites (New York: Wiley) 1968.
8. S.G. Bishop, U. Strom and P. Taylor, Phys. Rev. Lett, 34, 1346(1975).
9. M.D. Inngram, Phys. Chem. Glasses, 28,215 (1987).
10. M.K. Halima, W.M. Daud, and A. S. Zainal, Mater. Sci. Poland, 28. 137(2010).
11. A. A. Ali, Y. S. Rammah, and M. H. Shaaban, J. Non – Cryst. Solid, 514,52 – 59 (2019).
12. V. Rajendran, N. Planivelu, and K. Goswani, J. Non – Cryst. Solid, 320, 195 (2003).
13. P. Mošner, K. Vosejpková, and L. J. T. a. Koudelka, "Thermal properties and stability of TeO_2 containing phosphate glasses," vol. 522, no. 1-2, pp. 155-160, 2011.
14. O. Zamyatin, M. Churbanov, J. Medvedeva, S. Gavrin, E. Zamyatina, and A. J. J. o. N.-C. S. Plekhovich, "Glass-forming region and optical properties of the $\text{TeO}_2\text{-ZnO-NiO}$ system," vol. 479 ,pp. 29-41, 2018.
15. N .Elkhoshkhany, S. Y. Marzouk, and S. J. J. o. N.-C. S. Shahin, "Synthesis and optical properties of new fluoro-tellurite glass within ($\text{TeO}_2\text{-ZnO-LiF-Nb}_2\text{O}_5\text{-NaF}$) system," vol. 472, pp. 39-45, 2017.
16. N. Manikandan, A. Ryasnyanskiy, and J. J. J. o. N.-C. S. Toulouse, "Thermal and optical properties of $\text{TeO}_2\text{-ZnO-BaO}$ glasses," vol. 358, no. 5, pp. 947-951, 2012

17. V. Kamalaker, G. Upender, C. Ramesh, V. C. J. S. A. P. A. M. Mouli, and B. Spectroscopy, "Raman spectroscopy, thermal and optical properties of TeO₂–ZnO–Nb₂O₅–Nd₂O₃ glasses," vol. 89, pp. 149–154, 2012.
18. B. Chowdari, K. Tan, and F. J. S .S. I. Ling, "Synthesis and characterization of xCu₂O· yTeO₂·(1–x– y) MoO₃ glass system," vol. 113, pp. 711-721, 1998.
19. A. K. Measurement of band tails, optical energy gap, band positions, glass transition temperature and thermodynamic stability of some semiconducting oxide glasses. College of Education for pure science. of University of Kirkuk. 2022.
20. N. Sotani, K. Eda, M. Sadamatu, and S. J. B. o. t. C. S. o. J. Takagi, "Preparation and Characterization of Hydrogen Molybdenum Bronzes, H x MoO₃," vol. 62, no. 3, pp. 903-907, 1989.
21. N. Elkhoshkhany, M .Mahmoud, and E. S. J. C. L. Yousef, "STRUCTURAL, THERMAL AND OPTICAL PROPERTIES OF NOVEL OXYFLUOROTELLURIDE GLASSES," vol. 16, no. 6, 2019.